

Development of a quality control tool for phantoms of breast cancer screening using ImageJ

Naoki Kamiya

School of Information Science and Technology, Aichi Prefectural University, Nagakute, Aichi, Japan

Ryo Hirata

College of Media Arts, Science and Technology, University of Tsukuba, Tsukuba, Ibaraki, Japan

Norimitsu Shinohara

Department of Radiological Technology, School of Health Science, Gifu University of Medical Science, Seki, Gifu, Japan

Abstract- Mammography equipment requires routine quality control of the soft copy images. However, routine quality control is primarily conducted by visual evaluation, and numerous measurement locations are required even for semi-automatic methods using image processing software such as ImageJ, meaning that issues remain in time required to conduct this work, and quantifiability and replicability of measurement results. This study developed an ACR phantom quality control tool aimed at quantitative, highly replicable, and time-saving routine quality control of mammography equipment. The tool calculates contrast and CNR through automatic determination of the measurement area. With this tool, the user determines the reference point, and the relative value of the reference point is used to determine each measurement location. Measurements are then conducted before the measured values are used to calculate the mean values, CNR, and contrast of the measurement location. The tool was used to measure 40 days worth of image data taken of the same phantom, and calculate the mean pixel value, and the mean, distribution and standard deviation of the contrast and CNR of each measurement location for the 40 days. As a result, we confirmed that each of the values was within the normal range, and the tool was conducting accurate measurements. In addition, in quality control work for the ACR-endorsed phantom, when 3 participants were asked to perform ACR phantom measurement work using the tool as well as manually using ImageJ functions, the average working time using the tool was 16 sec, while manual work took 7 min 19 sec on average, meaning the tool took 1/29 of the time.

Keywords – Quality Control Tool, ACR phantom, ImageJ

I. INTRODUCTION

In Japan, the number of breast cancer patients is on the rise, and the incidence and mortality rates are extremely high [1]. With breast cancer, early detection is crucial, and over 90% of early detected cancers are curable. The main detection method for breast cancer is the use of dedicated breast X-ray equipment, with the 2 types of this being mammogram using mammography equipment, and ultrasound examination. Mammogram has the advantage of being able to detect cancer even when the breast tissue is large or thick, when ultrasound cannot reach, as well as very early detection of breast cancers that are difficult to find. Furthermore, comparison with past images enables understanding of tissue changes over time. Rapid digitalization of mammography devices is also occurring in recent years. Digitalization allows application of image processing and manipulation of images to make them suitable for radiographic image interpretation. Moreover, there is no need to develop the images taken, which means they can be preserved as data without the image deteriorating over time. Digitalization of mammography equipment is moving ahead for all of these reasons [2].

Current quality control of digital mammography equipment uses a simulated mammary tissue specimen phantom called an ACR phantom [3]. Routine photographs are taken of the phantom, and this image data is evaluated by sight [4, 5]. This study also uses an ACR phantom. Sight evaluation using the phantom is subjective, meaning that it can be swayed by factors such as the individual evaluator or the capacity of the display used for evaluation. This makes it difficult to conduct quantitative evaluation.

Research has been conducted using ImageJ to trial quantitative quality management to be used in place of the abovementioned sight evaluation for image data taken of the phantom [6]. This enables quantitative evaluation of routine quality control through image processing. Here, although quantitative measurement is achieved, the time

required is a problem, as there is a need to manually specify measurement areas on the ACR phantom, and 10 measurement locations are manually specified.

Our study develops a tool for automating measurement of ACR phantom contrast and contrast-to-noise ratio (CNR), which are routine quality control fields for soft copy diagnosis. This will enable time saving, greater replicability, and quantification in quality control.

II. OVERVIEW OF THE QUALITY CONTROL SYSTEM

2.1 *ImageJ and the development environment* –

The ACR phantom quality control tool developed in this study was created as an ImageJ plug-in. ImageJ is open source image analysis software developed by the US National Institutes of Health, and is used widely in medical practice. Plug-ins for ImageJ have been developed by various research institutions [7, 8].

As the ACR phantom that is the object of this study is used in standard accuracy control, by creating this system as an ImageJ plug-in, we aim to achieve quantitative quality control in the existing environment of medical practice. We used ImageJ ver 1.47m. In the future, we hope to publicly release the plug-in we have created and achieve our objective of time saving and quantification in quality control.

2.2 *ACR phantom measurement locations* –

The image data taken with the ACR phantom was in 10bit. The actual size of the phantom was 174.80 x 234.00 mm, and the image size was 3540 x 4740. The data format was DICOM. Images taken of the ACR phantom are given in Figure 1. The images in this figure are reduced of the full-scale image. Next, Figure 2 shows the measurement positions and measurement targets for each specimen from the ACR phantom. There were a total of 10 measurement locations, and the measurement targets consisted of every dot in the 3 simulated calcification specimens, the 3rd simulated tumor specimen, the acrylic disk, the transverse of the acrylic disk, and the center of the ACR phantom. These are the locations where measurement is currently conducted by sight/manually as described above, and they were thus used as the target locations for automated measurement in this study.

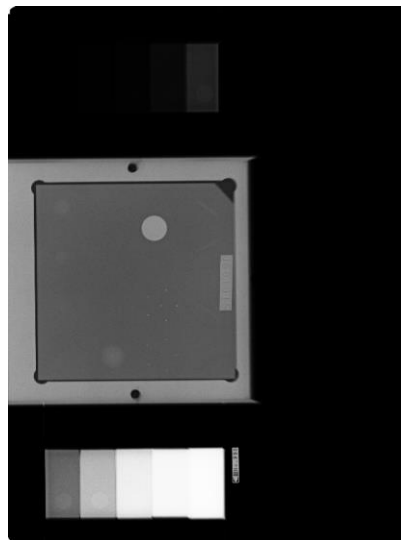


Figure 1. ACR phantom image

Given these targets, for the 3 simulated calcification specimens, the system set rectangular regions of interest (ROI) of 0.1 x 0.1 mm for each of 6 calcified dots. Similarly, a ROI of 2 x 2 mm was set for the 3rd simulated tumor specimen. Then, the means of the pixel values within each ROI were calculated. For the acrylic disk and the transverse of the acrylic disk, 4.5 x 4.5 mm ROIs were obtained, and the contrast was calculated using the ROI pixel values. For the center of the ACR phantom, ROI was similarly automatically set, and the CNR was calculated from the pixel value within the ROI.

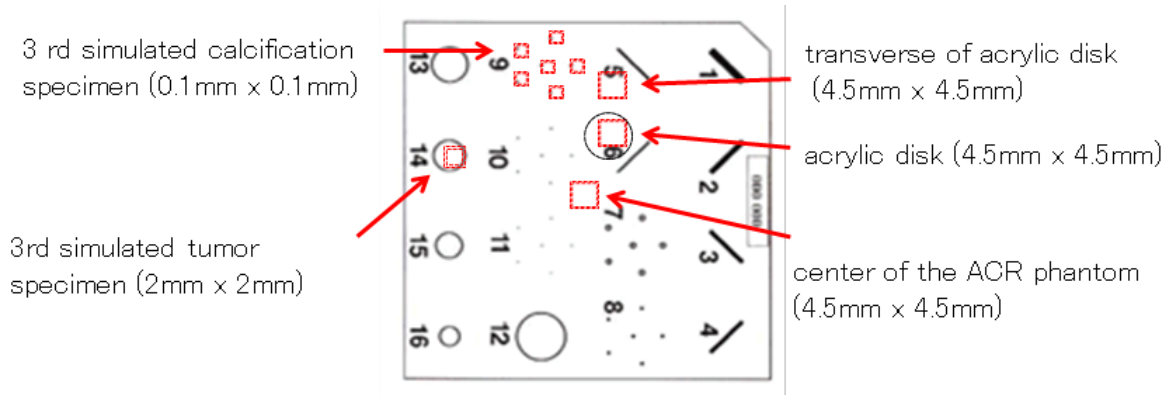


Figure 2. Measurement points and measurement targets for each specimen from the ACR phantom

III. METHOD

The automatic setting of measurement locations described above utilized the fact that the locational relationships of each specimen used as measurement targets within the phantom was invariable.

First, the user set a ROI for determining one reference point. Then, the reference point was calculated from the ROI set by the user, and using the relative values of that reference point, the ROI of each measurement target position was set, and automatic measurement was conducted of the pixel values of the measurement targets. Finally, using the measurement results, the mean, contrast, and CNR were calculated. A flow chart of the system is given in Figure 3.

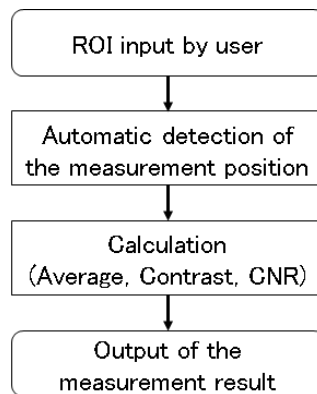


Figure 3. Flowchar of our proposed system

3.1 Reference point ROI input by the user –

With this system, the user sets the ROI that determines the reference point for the detection of each measurement location for the ACR phantom. Here, the target used for the calculation of reference points was a dot in the center of 1 simulated calcification specimen. This is because as this was the sample with the highest luminance (aside from the acrylic disk), there was high contrast with the background, making it easier to distinguish by sight. While the acrylic disk, with the highest luminance and largest area, seems the easiest choice, as its position within the phantom is not constant, it was deemed unsuitable as the reference point. Thus, the dot in the center of the simulated calcification specimen was used for determining the reference point.

For the reference point, a dot in the middle of one simulated calcification specimen was set as the center, and the central point was automatically calculated by the system from the ROI input by the user. The method for determining the central point of the dot in the center of the simulated calcification specimen was as follows.

First, the ROI was input by the user. Using the mouse, the user input an area that included only the center of the simulated calcification specimen. With this system, the coordinates of the upper left position where the mouse is clicked are given as (x, y) , and the coordinates of the lower right position when the mouse pointer is released are given

as (x_1, y_1) . The rectangle created by the diagonal lines between the 2 points was set as the ROI. Figure 4 shows the ROI input by the user for the simulated calcification specimen.

Next, the ROI is scanned and a rectangle of 0.25 x 0.25 mm is detected where the total of the luminance values taken from within the ROI is the highest. This is because a 0.05 x 0.05 mm rectangle is the equivalent of 1 pixel with the ACR phantom. Also, with ImageJ, the higher the luminance value, the smaller the pixel value. Therefore, in the program, the total pixel value is found for a 5 x 5 pixel area (total 25 pixels), and a rectangle is sought with the smallest total pixel value. Then, the coordinates of the center of the detected rectangle become the center of the simulated calcification specimen. Figure 5 shows the automatically selected area as a white rectangle.

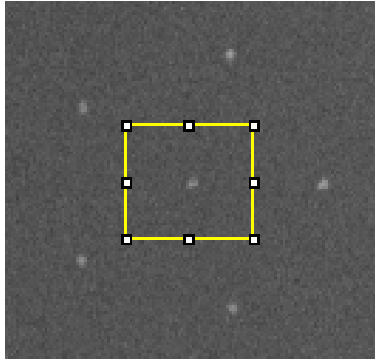


Figure 4. ROI input by the user for the simulated calcification specimen

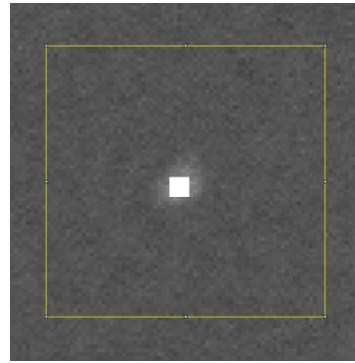


Figure 5. Automatically detected area as a white rectangle

3.2 Automatic detection of the measurement position –

Automatic detection of each ROI used the reference point found in the previous section. The relative locational relationships of each of the measurement locations are invariable. Here the difference between the coordinates of the upper left of each ROI and the coordinates of the reference point were calculated manually. This value was then used to determine each ROI that would become a measurement target. The relative value of each measurement location from the reference point is shown in Table 1.

Table -1 Relative value of each measurement location from the reference point (pixel)

	X coordinate	Y coordinate
3rd simulated calcification (1)	-402	-996
3rd simulated calcification (2)	-306	-861
3rd simulated calcification (3)	-400	-734
3rd simulated calcification (4)	-443	-861
3rd simulated calcification (5)	-556	-781
3rd simulated calcification (6)	-553	-939
3rd simulated tumor	-915	-450
Acrylic disk	-110	-723
Transverse of the acrylic disk	-110	-110
Center of the ACR phantom	-257	-255

3.2.1 ROI detection at locations where the measurement target is large –

With the ROI of the third simulated tumor sample, the acrylic disk, the side of the acrylic disk, and the center of the ACR phantom, the range that became the target of the measurement was comparatively larger than that of other ROI. Therefore, even if we consider error in the position of the reference point for the center of the simulated calcification sample, the ROI found from the reference point still lies well within the measurement target. Thus, the relative value from the reference point was used to determine the upper left coordinates of the ROI of the 3rd simulated tumor specimen, the transverse of the acrylic disk, and the center of the ACR phantom. Then, from the automatically set coordinates, 40 x 40 pixels was set as the ROI for the simulated tumor specimen, and 90 x 90 pixels for the acrylic disk and the transverse of the acrylic disk.

3.2.2 Simulated calcification specimen ROI detection –

With the 3 simulated calcification specimens, as the dot that serves as the measurement target is tiny, if the measurement area calculated from the reference point is set as the ROI, an area outside the simulated calcification

specimen is sometimes set as the ROI. When this happens, the measurement cannot be taken accurately. For this reason, the automatic ROI detection for the simulated calcification specimens used a different method to that for the abovementioned 3 locations.

For the simulated calcification specimens, the area surrounding the measurement location calculated from the reference point was scanned, and an accurate ROI was set. Here, a rectangular area was scanned of 20 x 20 pixels from the measurement position of each dot of the 3 simulated calcification specimens obtained from the reference point. The area of the ROI at this time considered the reference point error and the distance from other dots, and the ROI was set based on experience such that it would not include other dots if error occurred. Then, the ROI was scanned and a rectangle of 2 x 2 pixels was detected where there was the highest total luminance. The detected area became the ROI of the 3 simulated calcification specimens.

3.2.3 ROI detection for the acrylic disk –

For the acrylic disk, the positions within the ACR phantom were not constant. Therefore, when measurement positions were calculated using relative values from the reference point, there was a possibility that an area outside the acrylic disk would be set as the ROI. This meant it was necessary to conduct detection of the acrylic disk before setting the ROI for the measurement value calculation.

The detection of the acrylic disk took advantage of the fact that the size of the acrylic disk was invariable. First, from the measurement positions found using the relative values from the reference point, an area of 500 x 500 pixels was set as the measurement area for detecting the acrylic disk. Considering error in reference point and distance from other specimens, this size was set based on experience, as a size that would not include other specimens in the ROI even if error occurred. After determining the measurement area, a histogram was created within the measurement area. The histogram became bimodal, as it included both acrylic disk area and non-acrylic disk area.

Here, as acrylic disks are of approximately the same size, the total pixel value for searching was set at 38000 pixels, the pre-measured size of an acrylic disk. Then, searching began at the brightest pixel value and continued until the total pixel count reached 38000, and the pixel value p_1 that has the maximum number of pixels was found. For the non-acrylic disk area, searching was conducted from pixel value p_1 to the darkest pixel value, and the pixel value p_2 with the maximum number of pixels for the non-acrylic disk area was found. The total of both pixel values was divided by 2 and this became the threshold value. Then, using this threshold value, the measurement area was binarized. This allowed the detection of the acrylic disk. The center of gravity of the acrylic disk was calculated, and from this the ROI of the acrylic disk was calculated. The image binarized using the calculated threshold is shown in Figure 6. From Figure 6 we can see that the area of the acrylic disk was accurately detected.

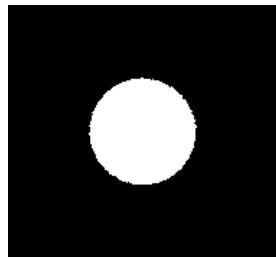


Figure 6. Automatically detected region of the acrylic disk

3.3 Evaluation value calculation –

With the ACR phantom quality control tool developed in this study, the program calculates the mean pixel value of each ROI, the ACR phantom contrast, and the CNR.

In image diagnosis using mammography, contrast is the most important field for lesion recognition. When diagnostic images are taken, the smaller the radiation dose the better, as this will have less impact on the patient's body. However, applying higher doses of radiation improves the quality of diagnostic images. For this reason, CNR is used as an objective indicator for achieving a balance between image quality and radiation dose.

CNR is an indicator of the ratio between contrast and noise, and the higher the contrast and lower the noise, the higher the CNR value. Images with higher CNR are said to be better images.

First, the mean value was calculated from the ROI of each measurement location found in the previous section. For this, the ROI was scanned, and the total pixel value found. Then, the total pixel value was divided by the ROI pixel number, and this was the mean value.

Next, for the acrylic disk and the transverse of the acrylic disk, the distribution required to calculate the CNR was found. The distribution was found by subtracting the mean of the squared pixel values from the square of the mean ROI pixel value. Next, the ROI was scanned, and the mean ROI pixel value and the mean of the squared ROI pixel value were found, and similarly the distribution of the acrylic disk and the transverse of the acrylic disk were found. Then, using the distribution and mean pixel values of the acrylic disk and transverse of the acrylic disk, the CNR and contrast were found. m_A , m_B represent the means, and σ_A , σ_B the standard deviation (the square root of the distribution) of the acrylic disk and transverse of the acrylic disk, respectively. These values were used in the following formula to calculate the CNR.

$$CNR = \frac{m_B - m_A}{\sqrt{\frac{\sigma_B^2 + \sigma_A^2}{2}}} \quad (1)$$

To calculate contrast, the following formula was used, with m_A , m_B as the mean values of the acrylic disk and transverse of the acrylic disk, respectively.

$$Contrast = \frac{m_B - m_A}{m_B + m_A} \quad (2)$$

3.4 Measurement result output –

With this system, when the user selects an area that includes the reference point as described in 3.1, and presses the measurement button at the bottom left of the screen, the file name, mean pixel value for each ROI, contrast, and CNR are output in a dialogue box. The output result is exported as text data, to be easily used in data analysis etc.

After the measurement, the area automatically recognized as the ROI is displayed as a white area, so that the ROI can be recognized visually. The results of automatic ROI recognition with the ACR phantom are given in Figure 7. Figure 8 is an enlarged view of the 3 simulated calcification specimens.

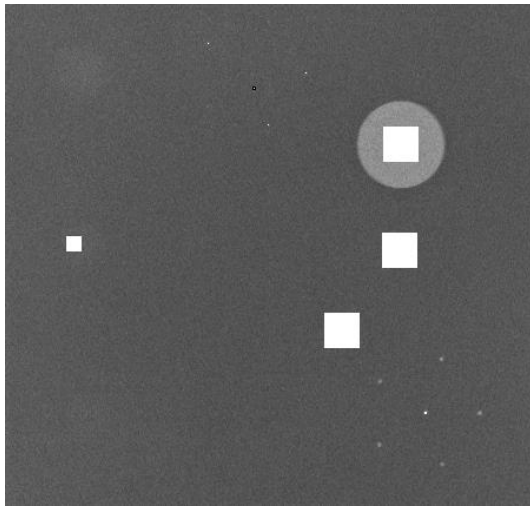


Figure 7. Automatic ROI detection results with the ACR phantom

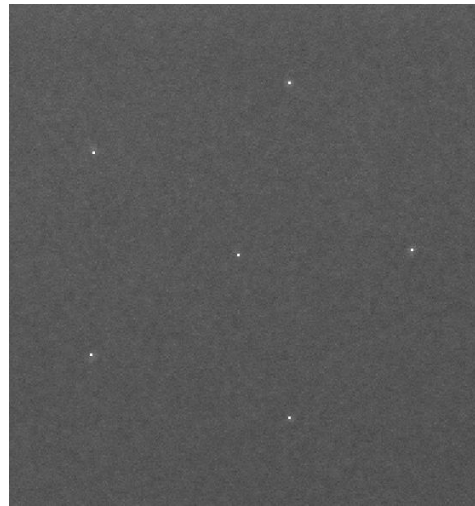


Figure 8. Enlarged image of the 3rd simulated calcification specimens and detected ROI

IV. EXPERIMENT

We tested whether or not the system we developed could be used in routine quality control work. To do so, we conducted an experiment to check that the measurement by the system was being carried out normally for each measurement location, as well as a comparative experiment, comparing the working time for ACR phantom quality control work when using the tool and when conducting the work manually using the functions of ImageJ.

4.1 Measurement value accuracy experiment –

In this experiment, relatively new mammography equipment with little wear was used, and 40 days worth of image data taken of the same phantom were the target of a measurement experiment.

4.1.1 Measurement of a simulated calcification specimen –

A test was conducted to determine whether the measurement of a simulated calcification specimen was being performed correctly. The simulated calcification specimen was comprised of 6 dots. The number of each dot is shown in Figure 10. The mean value of the ROI of each dot was found for the ACR phantom image data. This was repeated for 40 days worth of ACR phantom image data.

4.1.2 Measurement of other measurement targets –

We tested whether or not the measurement of the 3rd simulated tumor specimen, the acrylic disk, the transverse of the acrylic disk, and the center of the ACR phantom was being conducted accurately. Using the tool and the ACR phantom image data, the ROI mean value was found for the 3rd simulated tumor specimen, the acrylic disk, the transverse of the acrylic disk, and the center of the ACR phantom. This was repeated for 40 days worth of ACR phantom image data.

4.1.3 Measured values –

We tested whether or not the CNR and contrast were being calculated accurately. The ROI mean values and distributions measured with the tool, for the acrylic disk and the transverse of the acrylic disk, were used to calculate the CNR and contrast. This was repeated for 40 days worth of ACR phantom image data.

4.2 Comparative experiment of working time –

Here the working time required for ACR phantom quality control work using the system and manually using ImageJ were compared. For each, time was measured from opening ImageJ to the successful calculation of mean values, CNR, and contrast.

First, we will explain the method of measuring manually. The measurement locations are sufficiently expanded using the zoom function. Then, the measurement location is selected using the mouse. At this point, as it is deemed difficult for the user to accurately select the measurement area, the ImageJ ROI Manager function, Specify, is used to accurately set the ROI area. Then, the Measure function is used to calculate the ROI mean and distribution. This is repeated for all of the ACR phantom measurement locations. The CNR and contrast are also calculated, using the mean and standard distributions obtained from the measurement, and a calculator. This experiment was conducted with 3 highly computer literate participants.

V. RESULTS

5.1.1 Simulated calcification specimens –

The mean value for each dot on the simulated calcification specimens was measured using the system. The results of the measurements – the mean values, distribution, and standard deviation – for 40 days worth of data, are shown in Table 2. The standard deviations for 6 dots on 3 simulated calcification samples were 19.38, 14.9, 9.13, 15.04, 12.89, and 14.71.

Table -2 Results of the measurements – the mean values, distribution, and standard deviation – for 40 days worth of data

	Mean values	Distribution	Standard deviation
3rd simulated calcification (1)	557.89	375.5	19.38
3rd simulated calcification (2)	566.07	222.02	14.90
3rd simulated calcification (3)	598.98	83.31	9.13
3rd simulated calcification (4)	593.64	226.08	15.04
3rd simulated calcification (5)	578.17	166.20	14.71
3rd simulated calcification (6)	567.67	216.51	14.71

5.1.2 Measurement positions –

Using the system the mean values were measured for the 3rd simulated tumor specimen, the acrylic disk, the transverse of the acrylic disk, and the center of the ACR phantom. The mean, distribution, and standard deviation of 40 days worth of measurement results are given in Table 3. The standard deviation was 6.59 for the 3rd simulated tumor specimen, 6.14 for the acrylic disk, 4.89 for the transverse of the acrylic disk, and 5.01 for the center of the ACR phantom.

Table -3 The mean, distribution, and standard deviation of 40 days worth of measurement results

	Mean values	Distribution	Standard deviation
3rd simulated tumor	650.82	43.39	6.59
Acrylic disk	446.37	37.72	6.14
Transverse of the acrylic disk	683.40	23.63	4.89
Center of the ACR phantom	686.06	25.13	5.01

5.1.3 Image quality evaluation indicator measurement results –

The system was used to calculate the CNR and contrast of the ACR phantom. Table 4 gives the mean value, distribution, and standard deviation of the CNR and contrast for the 40 days. The standard deviation was 0.0033 for the contrast, and 0.0062 for the CNR.

Table -4 the mean value, distribution, and standard deviation of the CNR and contrast for the 40 days

	Mean values	Distribution	Standard deviation
Contrast	0.2098	1.08E-05	0.0033
CNR	0.41	3.78E-05	0.0062

5.2 Results of comparative experiment regarding working time measurement –

We measured the working time taken by each of the 3 experiment participants for measurement using the system and manual measurement. The results are given in Table 5. When the system was used, the average working time for ACR phantom quality control work was approximately 16 sec. On the other hand, manual measurement work conducted using ImageJ functions took an average of 7 min 19 sec.

Table -5 Average working time for ACR phantom quality control time

	Manual measurement (without our system)	With our proposed system
Participants 1	5m3s35	13s51
Participants 2	9m26s11	18s03
Participants 3	6m59s27	14s87

VI. DISCUSSION

6.1 Discussion of measured value accuracy experiment –

Let us focus on the standard deviation of the measured positions in experiment 4.1. The standard deviation of the 3 simulated calcification specimens was a larger value compared with that of the 3rd simulated tumor specimen, the acrylic disk, the transverse of the acrylic disk, and the ACR phantom, meaning that the measured values for the former specimens were more scattered. Here, the standard deviation of the simulated calcification specimens is considered to be within a normal range, because the mean of the ROI of these specimens used only a rectangle of 0.1 x 0.1 mm, i.e. a 2 x 2 pixel area (total 4 pixels), making the deviation more pronounced, and because the pixel value for the same positioning on the ACR phantom differs depending on the day and time the photographs were taken.

Next, the standard deviation of the acrylic disk, the transverse of the acrylic disk, the 3rd simulated tumor specimen, and the center of the ACR phantom, were 6.14, 4.89, 6.59, and 5.01, respectively. These are considered to be within a normal range, because the image data is displayed in 1024 gradation, and the pixel value of an area changes, even for the same phantom, depending on the time and day the image is taken.

Finally, the standard deviation of contrast and CNR were 0.0033 and 0.0062, respectively, meaning there was very little variation, and the measurements were taken well.

6.2 Comparison with results of manual measurement –

Using the results of 6.1, the relative values of the mean values were found. Three of the measurement targets – the 3 simulated calcification specimens, the 3rd simulated tumor specimen, and the center of the ACR phantom, were compared with the results of manual measurement in prior studies [9].

The relative value for the 3 simulated calcification specimens was approximately 3.4%. Meanwhile, for the manual measurement results, the relative value from the reference point for the simulated calcification specimens was within 5%. This means that the measurement by the system for the simulated calcification specimens was conducted accurately. Next, the relative value for each of the 3rd simulated tumor specimen and the center of the ACR phantom was less than 1.5%. Meanwhile, the relative value for the manual measurement results was close to 1, making the values extremely close. This means that the system was able to conduct measurements accurately.

6.3 Discussion of comparative experiment of working time –

The working time spent when using the system was 1/29 of that when measurement was conducted manually using the ImageJ functions, meaning that a large time saving was achieved compared with manual measurement. Further, measurement using the system required less complex operations than manual measurement using ImageJ functions, and measurement could be conducted smoothly even by users who had little experience with ImageJ. This means that user friendliness was greater than that for manual measurement.

Compared with current subjective quality management, this system objectively calculates values, and enables quality control that is not impacted by individual sight or the display used. Also, by automatically setting the ROI and automatically calculating the CNR and contrast of the ACR phantom, the working time required for ACR phantom quality control was reduced. Given the above, we believe this study has achieved its goal of quantifying routine quality control for mammography equipment, and reducing the working time required.

VII. CONCLUSION

This study successfully automated ACR phantom measurement for routine quality control of mammography equipment by developing a tool as a plug-in for ImageJ. In measurement location determination, the system took advantage of the fact that the positioning of each of the specimens in the ACR phantom was invariable. After the user inputs the ROI for the reference point determination, the relative value from the reference point already measured is used to determine the measurement locations. Based on the measured values, the tool we created then calculates the mean value, CNR, and contrast of each measured location, and outputs these results in a dialogue box.

Using this system, 40 days worth of ACR phantom images were measured. All of the measurement results were within normal range, and the system is considered to be conducting accurate measurements. Further, the working time required when the system was used was 1/29 of that required for manual measurement using ImageJ.

Given the above, we believe this study has achieved its goal of quantifying routine quality control for mammography equipment, and reducing the working time required. In the future, we believe it is necessary to measure images obtained with different X-ray radiation doses, in order to further test the effectiveness of the system.

REFERENCES

- [1] Ministry of Health, Labour and Welfare, JAPAN “Vital Statistics in JAPAN –The latest trends–”, <http://www.mhlw.go.jp/english/database/db-hw/vs01.html>, accessed Aug. 1, 2015.
- [2] H. P. Chan, L. T. Niklason, D. M. Ikeda, K. L. Lam, D. D. Adler, “Digitization requirements in mammography: Effects on computer - aided detection of microcalcifications”, *Medical physics*, vol. 21, no. 7, pp. 1203-1211, 1994.
- [3] American College of Radiology, “Mammography quality control manual”, New York, 3, 1999.
- [4] D. P. Chakraborty, M. P. Eckert, “Quantitative versus subjective evaluation of mammography accreditation phantom images”, *Medical Physics*, vol. 22, no. 2, pp.133-143, 1995.
- [5] K. W. Brooks, J. H. Trueblood, K. J. Kearfott, D. T. Lawton, “Automated analysis of the American College of Radiology mammographic accreditation phantom images”, *Medical physics*, vol. 24, no. 5, pp. 709-723, 1997.
- [6] Y. Lee, D. Y. Tsai, N. Shinohara, “Computerized quantitative evaluation of mammographic accreditation phantom images”. *Medical physics*, vol. 37, no.12, pp. 6323-6331, 2010.
- [7] M. Hachet - Haas, N. Converset, O. Marchal, H. Matthes, S. Gioria, J. L. Galzi, S. Lecat, “FRET and colocalization analyzer–A method to validate measurements of sensitized emission FRET acquired by confocal microscopy and available as an ImageJ Plug - in”, *Microscopy research and technique*, vol. 69, no. 12, pp. 941-956, 2006.
- [8] National Institute of Health, “ImageJ Plugins”, <http://rsb.info.nih.gov/ij/plugins>, accessed Aug. 1, 2015.
- [9] N. Shinohara, E. Katagiri, M. Tanaka, “Proposal of routine quality control items for the soft copy diagnostic”, *J. Jpn. Assoc. Breast Cancer Screen.*, vol.21, no.3, p.471, 2012. (in Japanese)